Polariton Mott insulator with trapped ions or circuit QED

M. Hohenadler,[1,*] M. Aichhorn,[2] L. Pollet,[3] and S. Schmidt[3]

[1]*Institut für Theoretische Physik und Astrophysik, Universität Würzburg, D-97074 Würzburg, Germany*

[2]*Institut für Theoretische Physik–Computational Physics, TU Graz, A-8010 Graz, Austria*

[3]*Institut für Theoretische Physik, ETH Zurich, CH-8093 Zurich, Switzerland*

(Received 14 October 2011; published 9 January 2012)

We consider variants of the Jaynes-Cummings-Hubbard model of lattice polaritons, taking into account next-nearest-neighbor, diagonal, and long-range photon hopping in one and two dimensions. These models are relevant for potential experimental realizations of polariton Mott insulators based on trapped ions or microwave stripline resonators. We obtain the Mott-superfluid phase boundary and calculate excitation spectra in the Mott phase using numerical and analytical methods. Including the additional hopping terms leads to a larger Mott phase in the case of trapped ions, and to a smaller Mott phase in the case of stripline resonators, compared to the original model with nearest-neighbor hopping only. The critical hopping for the transition changes by up to about 50 percent in one dimension and by up to about 20 percent in two dimensions. In contrast, the excitation spectra remain largely unaffected.

DOI: 10.1103/PhysRevA.85.013810 PACS number(s): 42.50.Pq, 42.50.Ct, 71.36.+c, 73.43.Nq

I. INTRODUCTION

The study of strongly correlated and condensed phases of ultracold atoms has become an extremely active and versatile research field over the last decade. It has been triggered by the experimental realization of a Mott insulator to superfluid quantum phase transition of neutral atoms in an optical lattice [1] as described by the seminal Bose-Hubbard model [2]. The recent realization of strong light-matter interaction in various cavity-quantum electrodynamics (QED) systems has triggered an immense interest in realizing strongly correlated and condensed phases with photons as well. Bose-Einstein condensation and superfluidity of weakly interacting polaritons, i.e., quasiparticles that form when photons strongly interact with matter, have already been observed experimentally with exciton polaritons in a quantum well coupled to a photonic crystal cavity [3].

Today, a key challenge is to reach the limit of strong correlations, that is, a photonic or polaritonic Mott insulator [4–6]. The Jaynes-Cummings-Hubbard model (JCHM) has been introduced to describe such an extreme state of light in an array of coupled high-Q electromagnetic resonators [4]. In the generic JCHM, photons hop between nearest-neighbor (nn) cavities and interact with a single two-level system locally in each cavity. This fundamental light-matter coupling introduces a nonlinearity into the system, leading to an effective repulsive photon-photon interaction. The competition between hopping (delocalization) and light-matter interaction (localization) leads to a phase diagram featuring Mott lobes similar to the Bose-Hubbard model. The phase diagram, excitations, and critical exponents of the generic JCHM have been studied theoretically using various numerical and analytical methods [4–15] and it has been shown that the same critical theory applies to the JCHM and Bose-Hubbard model [10–12,15]. Original proposals for an experimental realization of the JCHM were based on nitrogen vacancy centers in diamond [4] or self-assembled quantum dots in photonic crystals [16]. However, both variants suffer from short coherence times and are prone to disorder effects.

Two rather recent proposals, which are not limited with respect to decoherence and disorder, are based on circuit QED [10,17,18] and trapped ions [19,20]. In circuit QED, Josephson qubits are coupled to stripline resonators. Arrays can be formed by capacitively coupling resonators in one-dimensional (1D) or two-dimensional (2D) geometries. In trapped ions, the role of photons is played by phonon excitations which are exchanged between the ions, and arrays can be formed either in linear Paul traps or in microtraps. However, in both cases, photon transfer beyond the canonical nn hopping cannot be neglected. In a circuit-QED setup, the 2D square lattice geometry gives rise to next-nearest-neighbor (nnn) hopping. In the case of trapped ions, hopping is mediated by the Coulomb interaction between dipoles and is, thus, long-range in all lattice dimensions. An accurate quantitative description of the Mott-superfluid transition in these systems requires more general versions of the JCHM. In this paper, we show that additional hopping terms substantially modify the Mott-superfluid phase boundary. We compare exact numerical results obtained from extensive quantum Monte Carlo (QMC) simulations with the variational cluster approach (VCA) and analytical calculations based on a linked-cluster expansion.

The paper is organized as follows. In Sec. II, we introduce the JHCM with a general hopping term and specify the cases pertaining to circuit-QED arrays and trapped ions. In Sec. III, we outline the numerical and analytical methods used. Section IV contains a discussion of our results for the effect of additional hopping terms on the phase diagram and the elementary excitations. A summary is given in Sec. V. Finally, the Appendix contains relevant results for the atomic limit.

II. MODELS

The JCHM is defined by the Hamiltonian

$$\hat{H} = \sum_i h_i^{\mathrm{JC}} + \sum_{ij} t_{ij}(a_i^\dagger a_j + \mathrm{H.c.}) - \mu\hat{N}, \qquad (1)$$

*martin.hohenadler@physik.uni-wuerzburg.de

with the on-site JC Hamiltonian for the cavity at site i of the lattice,

$$h_i^{\mathrm{JC}} = \omega_{\mathrm{b}} a_i^\dagger a_i + \omega_{\mathrm{q}} \sigma_i^+ \sigma_i^- + g(\sigma_i^+ a_i + \sigma_i^- a_i^\dagger). \qquad (2)$$

Here, ω_{b} denotes the energy of bosons (photons or phonons), and ω_{q} is the level splitting of the qubits (ions or Josephson qubits). The spin operators $\sigma^\pm$ describe intrasite transitions between the two qubit levels induced by emission or absorption of a boson with rate g. The bosonic operators a and $a^\dagger$ fulfill the usual commutation relations $[a_i, a_j^\dagger] = \delta_{ij}$. The coupling g gives rise to the formation of polaritons (combined boson-qubit excitations) whose number operator $\hat{N} = \sum_i (a_i^\dagger a_i + \sigma_i^+ \sigma_i^-)$ commutes with $\hat{H}$. Hence, within this theoretical framework, the polariton number is conserved and can be controlled via the chemical potential μ.

The second term in Eq. (1) describes photon hopping between site i and site j of the cavity array with amplitude t_{ij}. At this point, the hopping is completely general and may involve any pair of lattice sites. In previous work, only nn transfer along the directions of the lattice basis vectors was considered, with $t_{ij} = -t$. We refer to this case as the *original* JCHM in the following.

Here we consider the JCHM with more complex hopping terms, motivated by possible realizations using trapped ions in 1D Paul traps and stripline resonators on a 2D square lattice.

A. Trapped ions

The case of trapped ions implies a 1D model with frustrated long-range hopping,

$$t_{ij} = t \frac{(-1)^{|i-j|}}{|i-j|^3}, \qquad (3)$$

arising from dipole-dipole interactions between confined ions [19]. Here, t denotes the nn hopping strength. The effects of long-range hopping for trapped ions have been investigated using simple mean-field-like approximations [20]. However, the validity of mean-field theory in such a 1D setting is not clear. In particular, it fails to predict the Kosterlitz-Thouless transition at the tip of the Mott lobe, which manifests itself as a nonanalytic cusp in the phase boundary [7,21]. In this paper, we therefore address this problem using numerical methods.

Due to the alternating sign in Eq. (3), which gives rise to frustration, QMC simulations are impracticable. Instead, we use the VCA, a quantum cluster method which can be applied to frustrated systems and also to compute single-particle excitation spectra. To benchmark the VCA for the case of long-range hopping, we also present results for the case

$$t_{ij} = \frac{t}{|i-j|^3}, \qquad (4)$$

i.e., without the alternating sign. Hamiltonian (1) with the hopping integrals given by Eq. (4) can be studied using QMC simulations to obtain the exact phase boundary for the Mott-superfluid transition.

B. Stripline resonators

The 2D JCHM may be realized in experiments using stripline resonators on a square lattice. A simple configuration is shown in Fig. 1. The hopping integral $t_{ij} = -t$ when i and j are nn's along a lattice bond (as in previous studies of the 2D JCHM) and $t_{ij} = -t'$ for diagonal nnn's on every other plaquette. For any other pair of lattice sites we have $t_{ij} = 0$.

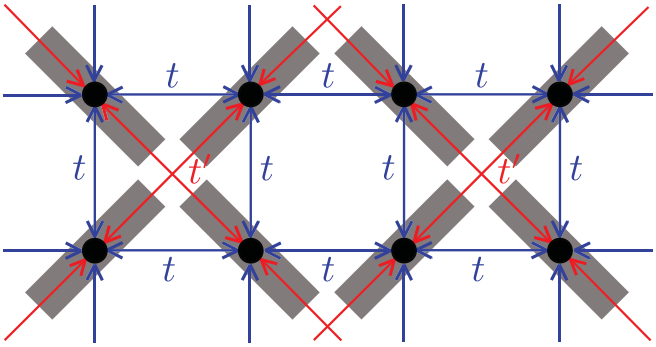

FIG. 1. (Color online) Circuit-QED realization of the JCHM on a 2D square lattice. A filled circle indicates a lattice site, defined by the position of a qubit. Each qubit is located inside a resonator represented by a rectangle. The capacitive coupling between resonators gives rise to photon hopping across the lattice. Two different couplings occur: nearest-neighbor hopping, with amplitude t along the lattice axes; and diagonal next-nearest-neighbor hopping, *in every other* plaquette with amplitude t'.

In this circuit QED setup, the hopping rates t and t' are proportional to the mutual capacitances of the resonators in Fig. 1 [17,22]. By choosing a proper geometry and/or distance between pairs of resonators on the diagonal of the array (determining t') and pairs of resonators on the lattice axes (determining t), the diagonal hopping rate t' can be made much smaller with respect to the nn hopping rate t, and vice versa. Thus, the ratio t'/t can be engineered almost arbitrarily [23]. Here we consider the ratio $t'/t = 1/2$.

The freedom to tune the ratio t'/t to substantial values in circuit-QED systems is in strong contrast to ultracold atoms in optical lattices. For the latter, hopping integrals beyond nn pairs are orders of magnitude smaller [24]. Moreover, diagonal hopping is absent on hypercubic lattices because of the orthogonality of the Wannier states. The small size of hopping integrals beyond the nn terms makes their effect very small, with correspondingly few studies available [23,25].

The circuit-QED model with hopping integrals t and t' as depicted in Fig. 1 can be simulated using the QMC method. For comparison, we also present results for a 2D model with nn hopping t and nnn hopping t'' between sites separated by two lattice constants, along the (1,0) and (0,1) directions.

III. METHODS

This section describes the methods used in this work in some detail. In two dimensions, we use exact QMC simulations, the VCA, and an analytical linked-cluster approximation around the mean-field limit in two dimensions. Since mean-field theory is not a valid starting point for an expansion in one dimension, we show only numerical results (QMC, VCA) for that case.

A. Quantum Monte Carlo

In the absence of frustration, bosonic Hamiltonians of the form of (1) can be studied by exact QMC simulations.

A particularly popular representation is the continuous-time stochastic series expansion [26]; it has been applied to the JCHM model before [9,15,27]. We use the ALPS 1.3 implementation [28] of the stochastic series expansion with directed loop updates [29–31]. A maximum site occupation of six photons is sufficient to make the truncation error negligible. The long-range hopping defined by Eq. (4) is treated by taking into account all transfer processes with $|i-j| \leqslant L/2-1$ for system size L (due to periodic boundary conditions).

The Mott-superfluid phase boundary can be determined by calculating the superfluid density

$$\rho_{\mathrm{s}} = \frac{\langle w^2 \rangle}{\beta D L^{D-2}}, \tag{5}$$

where D denotes the dimension of the lattice, w is the winding number [32], and β is the inverse temperature. Exploiting the scaling form of ρ_s [2], the critical point can be obtained from simulations with different system sizes at inverse temperature $\beta/L^z = \text{const}$. The dynamical critical exponent of the JCHM is $z=1$ for the fixed-density transition and $z=2$ for the generic transition [15]. For large enough values of the system size L, curves for different L values intersect at a single point [9,15] which defines t_{c} (for horizontal scans in the t,μ phase diagram) respectively μ_{c} (for vertical scans). We use system sizes up to $L=64$ in one dimension and up to 40×40 for the 2D models. The inverse temperatures were typically $\beta/L^2 = 1/4$ for $z=2$ and $\beta/L = 2$ or 4 for $z=1$. The resulting accuracy for the phase boundary in units of g is estimated to be better than 0.0005 (below the symbol size used in the figures).

B. Variational cluster approach

The minus-sign problem resulting from the frustration induced by choice (4) for the hopping integrals motivates the use of an alternative numerical method. The VCA is a cluster method; hopping within a finite reference cluster is treated exactly, and hopping beyond the cluster is taken into account perturbatively. For the relation to other popular cluster methods such as the dynamical mean-field theory, see [33]. The VCA [33] can be applied for any choice of hopping integrals in one and two dimensions and, also, permits calculation of excitation spectra. It has been applied to the original JCHM with $t'=0$ in [8] and [34], where, in the latter case, the problem was mapped to an effective model. In one dimension, the VCA yields quantitatively reliable results [8,34]. In 2D, accurate results can be obtained except for a small region around the Mott lobe tip in the phase diagram.

The quality of the approximation depends on the size of the cluster, compared to the correlation lengths of the problem, and the number of variational parameters. Since larger clusters and more parameters have comparable impacts, we use only the boson energy in the cluster as a parameter and vary the cluster size. This is also motivated by the presence of long-range hopping terms in the models considered here. For more details see [8].

Here we investigate Hamiltonian (1) using the VCA in its formulation for bosonic systems [35]. We work exclusively at zero temperature. To deal with the long-range hopping defined by Eqs. (3) and (4), we allow for hopping processes up to a distance $L-1$, where L is the cluster size used in the calculation.

On the technical side, we note that care is required when carrying out the sums over wave vectors in the calculation of the grand potential [8,33]. Far from the lobe tip, the sums converge rapidly, whereas close to the tip, an increasingly finer mesh is required. We attribute this effect to the momentum dependence of the self-energy and excitations. Deep in the Mott phase, the particle and hole bands are almost completely flat, whereas close to the lobe tip, they acquire a substantial dispersion [8]. Given convergence, the VCA yields the correct form of the phase boundaries, leading to improved results for the 2D case compared to exact QMC data [8,9].

C. Linked-cluster expansion

We analytically calculate the photonic Matsubara Green's function $G_{ij}(\tau;\tau') = -\langle \mathcal{T} a_i(\tau)\bar{a}_j(\tau')\rangle$ with the time-ordering operator $\mathcal{T}$ and $\bar{a}_j(\tau') = e^{H\tau'} a_j^\dagger e^{-H\tau'}$ using a linked-cluster expansion in terms of local cumulants originally developed by Metzner [36] for the Fermi-Hubbard model and recently applied to the Bose-Hubbard model [37] and the JCHM [12]. After a Fourier transformation and analytic continuation, the inverse Green's function directly yields the excitation spectrum $\omega(\mathbf{k})$ via $G^{-1}(\mathbf{k},\omega)=0$ and the phase boundary $t_c(\mu)$ via $G^{-1}(\mathbf{0},0)|_{t_c(\mu)} = 0$. Key results are summarized below.

1. *Random phase approximation*

Within the mean-field random phase approximation (RPA), the full Green's function is given by [11]

$$G(\mathbf{k},\omega) = \frac{G^0(\omega)}{1 - J(\mathbf{k})G^0(\omega)}, \tag{6}$$

with the local one-particle cumulant

$$G^0(\omega) = \sum_{\sigma=\pm} \frac{z_{n+1}^{-,\sigma}}{\Delta_{n+1}^{-,\sigma} - \omega} - \frac{z_n^{\sigma,-}}{\Delta_n^{\sigma,-} - \omega}. \tag{7}$$

The hole or particle spectral weights and bare excitation energies in the numerator and denominator in Eq. (7) are given in the Appendix. In Eq. (6), $J(\mathbf{k})$ denotes the bare dispersion. For the 2D circuit QED model in Fig. 1,

$$J(\mathbf{k}) = 2t(\cos k_x + \cos k_y) + 2t' \cos k_x k_y. \tag{8}$$

From Eq. (6), we can derive analytical expressions for the phase boundary and the excitation spectrum. For example, the RPA phase boundary for the t,t' model at a fixed ratio $R = t'/t$ is given by $1/t_c = 4G^0(0)(1+R/2)$. Thus, on the mean-field level, nnn hopping simply rescales the nn hopping according to $t_c \mapsto t_c/(1+R/2)$. Hence, a positive (negative) nnn hopping decreases (increases) the size of the Mott lobes and makes mean-field theory a better (worse) approximation. The RPA is equivalent to the cluster perturbation theory (VCA without variational parameters) for a single-site cluster [35].

2. *One-loop approximation*

The mean-field RPA corresponds to a summation of all self-avoiding walks through the lattice. In order to take into account the leading quantum correction, one can additionally include all one-time forward/backward hopping processes

between two neighboring sites. The resulting so-called *one-loop approximation* was previously found to be in excellent agreement with numerical results for the phase diagram for both the Bose-Hubbard model [37] and the original JCHM (1) with $t' = 0$ [11].

IV. RESULTS

To calculate the phase diagram of the models discussed in Sec. II, we vary the nn hopping strength t common to all models and scale any additional hopping integrals accordingly. In the following, we use g as the unit of energy and consider $\omega_b = \omega_q = 1$ (resonance condition). We also set $\hbar$, k_B, and the lattice constant to 1.

A. Mott-superfluid transition

Similarly to cold atoms in optical lattices, the JCHM can be tuned across the Mott-superfluid transition by changing the ratio t/g. We therefore expect the additional hopping terms discussed in Sec. II to modify the extent of the Mott insulating region in the phase diagram. Because the Mott phase is of particular interest as an initial state for possible applications in quantum computing and quantum information, we determine the size of the first (largest) Mott lobe with polariton density $n = 1$.

1. One dimension

We begin with the 1D model with long-range hopping given by Eq. (4), which represents an interesting theoretical problem for two reasons. First, it allows us to benchmark the VCA against exact QMC results for the novel case of long-range hopping. Second, the long-range hopping is expected to mimic the effect of increasing the lattice coordination Z, while keeping the lattice topology and dimension unchanged. Previous VCA calculations for the JCHM have demonstrated a crossover from Kosterlitz-Thouless behavior (reflected in a strongly nonparabolic shape of the phase boundary, including re-entrant behavior [21]) on a 1D chain to a mean-field like, parabolic phase boundary for the 2D square lattice [8]. This crossover is also visible upon comparing Figs. 2 and 3. Mean-field behavior in a 1D matter-light system is also suggested by results for a two-component Bose-Hubbard model coupled to a global photon mode (as in the Dicke model) [38]; the coupling gives rise to photon-mediated long-range interaction.

Figure 2(a) shows the Mott-superfluid phase boundary for the first Mott lobe. The long-range hopping substantially reduces the extent of the insulating phase, compared to the original JCHM (shaded regions; results taken from [7]). Due to the particular shape of the phase boundary in one dimension, the reduction of the critical hopping due to t_{ij} can be very large, about 50 percent for $\mu/g = 0.1$.

The Kosterlitz-Thouless phase transition at a fixed polariton density, which occurs at the tip of the Mott lobe, is difficult to study by the QMC method. Away from the lobe tip, the critical points from QMC agree well with the VCA results. The approximate cluster approach underestimates the effect of quantum fluctuations for larger t/g, leading to a slightly larger Mott phase than found by QMC as visible in Fig. 2(a) for the QMC data points located at $t/g \gtrsim 0.1$. This finding is in

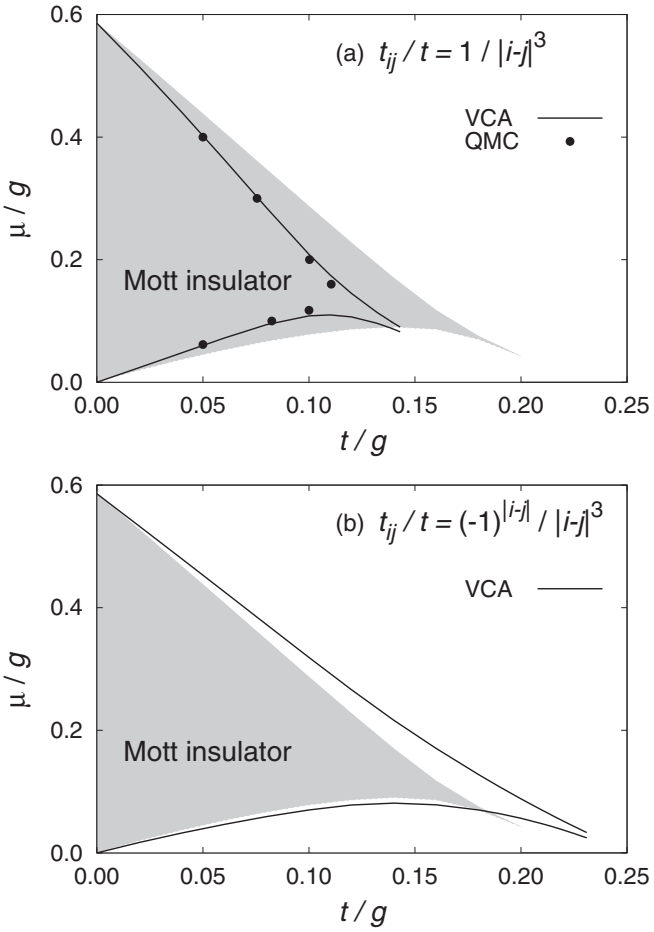

FIG. 2. Zero-temperature Mott lobe with density $n = 1$ of the 1D JCHM, showing the effect of (a) long-range hopping defined by Eq. (4) and (b) sign-alternating long-range hopping defined by Eq. (3), as appropriate for an experimental realization based on trapped ions. Case (a) can be investigated by QMC simulations (symbols), and the phase boundary is compared to the VCA (lines; for a cluster size $L = 8$). For reference, we also show the exact result for the original JCHM with nearest-neighbor hopping only [7] (shaded regions). Case (b) is not accessible for QMC, and we rely on the VCA for the phase diagram.

accordance with the cluster size dependence of the VCA Mott lobe in [8], where satisfactory convergence was achieved for $L = 8$ (the same size as used here). Far away from the lobe tip, for $t/g < 0.1$ in Fig. 2(a), the transition is essentially driven by density fluctuations, and the VCA and QMC results agree almost perfectly.

Concerning a possible change of the universality class in the presence of long-range hopping, neither the QMC nor the VCA results provide any evidence of such a scenario. The shape of the Mott lobe for the model with long-range hopping is reminiscent of the phase boundary of the original JCHM (shaded region). Besides, the QMC results for the superfluid density (not shown) exhibit scaling with dynamical critical exponent $z = 1$. The absence of mean-field behavior despite long-range hopping is a consequence of the fast decay with distance, $t_{ij} \sim |i - j|^{-3}$; see Eq. (4).

Turning to the model for trapped ions, with sign-alternating long-range hopping as given by Eq. (3), we note that the QMC

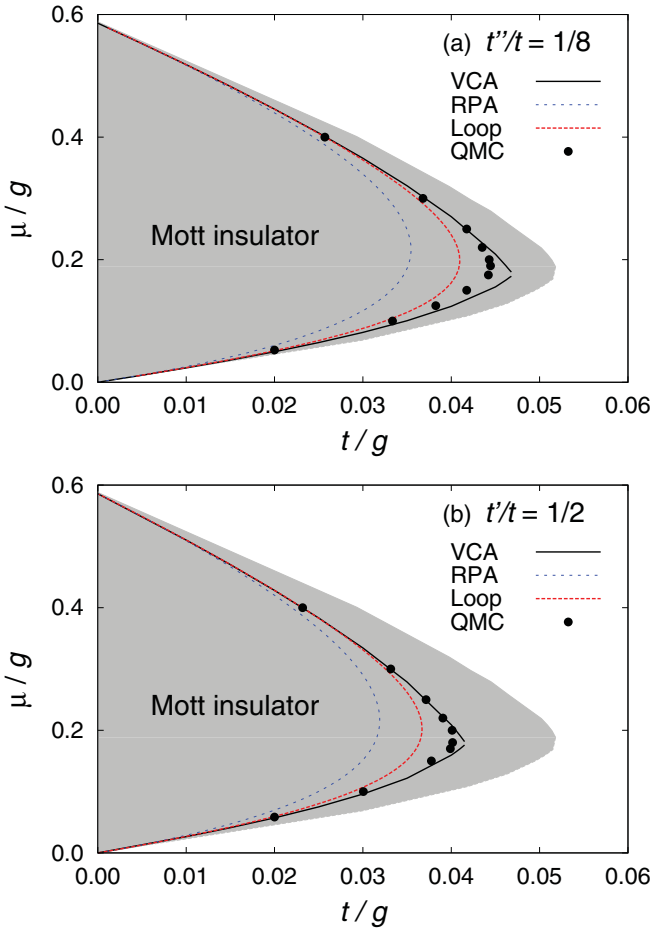

FIG. 3. (Color online) Zero-temperature Mott lobe with density $n = 1$ of the 2D JCHM, showing the effect of (a) next-nearest-neighbor hopping $t'' = t/8$ (see Sec. II) and (b) *diagonal* next-nearest-neighbor hopping $t' = t/2$ as appropriate for an experimental realization based on stripline resonators (see Fig. 1 and Sec. II). We show results from QMC simulations (symbols), the VCA (lines; $L = 8$), the mean-field theory (RPA), and the one-loop approximation. For reference, we also include the $t' = t' = 0$ QMC results for the original 2D JCHM model (shaded regions; taken from [9]).

method suffers from a severe minus-sign problem. Relying on the accuracy of the VCA established in Fig. 2(a) and in previous work, we show the VCA phase boundary in Fig. 2(b). The sign-alternating hopping has an effect opposite to the choice (4). The extent of the Mott is noticeably increased compared to the model with nn hopping only. The largest change of the critical hopping again occurs for $\mu/g \approx 0.1$, with an increase of about 50 percent. The qualitative shape of the phase boundary is unchanged.

2. *Two dimensions*

We now turn to the results for the 2D models discussed in Sec. II. Since there is no frustration in either case, we can study the Mott-superfluid transition exactly using the QMC method. The findings are compared to the VCA and to analytical approximations.

Figure 3(a) contains the results for the t,t'' model, with $t''/t = 1/8$ [motivated by taking a $1/r^3$ dependence as in Eq. (4) but keeping only the first two terms]. The hopping t'' causes a 10 percent reduction of the critical hopping close to the tip compared to the model with nn hopping only [9]. The VCA provides a remarkably good description of the whole phase boundary. In particular, the spurious inflection points visible in earlier work [8,9] are absent. As in one dimension, the underestimation of spatial fluctuations leads to slightly larger values of the critical hopping for the Mott-superfluid transition. Conversely, the RPA mean-field result severely underestimates the effect of fluctuations, a deficiency which is, to a large extent, remedied within the one-loop approximation.

Results for the 2D circuit QED model with hoppings $t'/t = 1/2$ are shown in Fig. 3(b). The effect of t' is qualitatively very similar to that in Fig. 3(a), with the larger value of t' compared to t'' leading to a stronger reduction of the critical hopping close to the tip (about 20 percent). The agreement between the different methods, in particular, the VCA and QMC, is even better than for the t,t'' model. Hence, except for details such as critical exponents [15], both the VCA and the one-loop approximation may be used for semiquantitative analyses of the 2D JCHM at substantially smaller computational cost than for the QMC.

B. Excitation spectra

Single-particle excitation spectra are directly accessible in cavity QED via photoemission spectroscopy. As demonstrated previously [8,12,27], they allow us to identify the system state via the presence or absence of a Mott gap and to calculate effective particle and hole masses. We therefore study here the effect of the additional hopping processes in models for trapped-ion and circuit-QED realizations of the JCHM.

Figure 4 compares the excitation spectrum deep in the Mott phase for the cases of the original 1D JCHM [Fig. 4(a)] and the model with sign-alternating long-range hopping [Fig. 4(b)]. Results were obtained using the VCA. The four gapped branches of the original model persist in the presence of long-range hopping; the two low-lying branches correspond

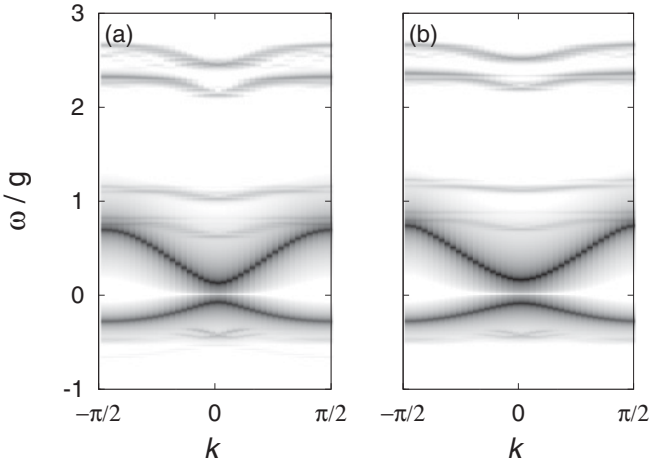

FIG. 4. Zero-temperature excitation spectra of the 1D JCHM at zero detuning with (a) nearest-neighbor hopping t and (b) sign-alternating long-range hopping t_{ij}, relevant for trapped ions Eq. (3). Results are from the VCA with cluster size $L = 8$ and using $t/g = 0.1$, $\mu/g = 0.15$ [see Fig. 2(b)].

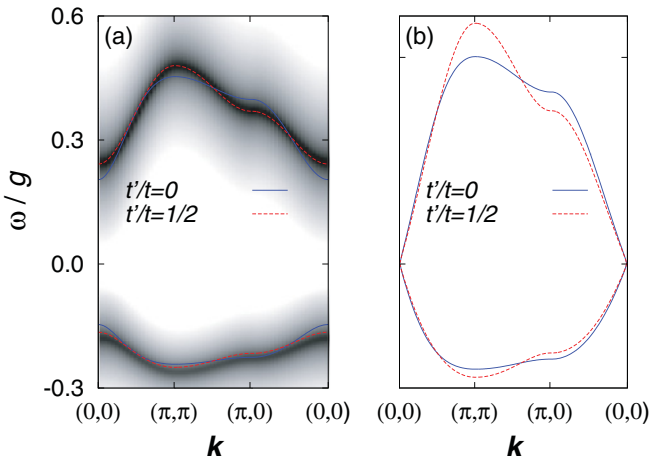

FIG. 5. (Color online) Zero-temperature excitation spectra for the 2D JCHM at zero detuning with $t' = 0$ (solid lines) or $t'/t = 1/2$ [dashed lines and intensity plot in (a)], as appropriate for a circuit-QED setup (see Fig. 1 and Sec. II). (a) Parameters deep in the Mott lobe, using $t/g = 0.02$, $\mu/g = 0.22$. (b) Parameters exactly at the Mott lobe tip, using $t/g = 0.04$ (for $t' = 0$) respectively $t/g = 0.032$ (for $t'/t = 1/2$) and $\mu/g = 0.22$ [see Fig. 3(b)]. Lines are RPA results for the particle/hole dispersion. The density plot in (a) shows VCA results based on a 2×2 cluster.

to conventional particle/hole excitations [8], whereas the high-energy branches are so-called conversion modes, which arise from the composite nature of polaritons [11]. The upper modes have a very small bandwidth and low spectral weight. Comparing Figs. 4(a) and 4(b), we conclude that the effect of long-range hopping is negligible. A comparison close to the lobe tip is difficult in one dimension, because of the different extent of the Mott phases [see Fig. 2(b)].

Results for the excitation spectra of the 2D circuit-QED model are shown in Fig. 5, focusing on low-energy modes. Deep in the Mott phase, we find perfect agreement between the VCA and the RPA. The renormalization of the Mott-superfluid transition (including the Mott gap) due to t' [see Fig. 3(b)] is visible from the particle and hole bands close to the $\mathbf{\Gamma}$ point.

Finally, we consider the spectrum exactly at the lobe tip. Because our formulation of the VCA is restricted to the gapped Mott phase, we show only the corresponding RPA results in Fig. 5(b). The ratio t/g has been tuned to the lobe tip for both $t' = 0$ and $t' > 0$. The RPA dispersion becomes relativistic, with gapless, linear modes in both cases and noticeable differences due to t' only far away from the Γ point and, hence, at high energies. In particular, the sound velocities are practically identical. The presence of linear excitations at the lobe tip is a signature of the fixed-density transition with dynamical critical exponent $z = 1$. The value $z = 1$ has recently been demonstrated using QMC simulations [15,39] for the case $t'' = t' = 0$ (original JCHM). As expected, the universality does not change in the presence of additional hopping terms.

V. SUMMARY

We have investigated the effects of additional hopping terms beyond the generic nn transfer in the JCHM in one and two dimensions. Such hopping terms arise when considering possible experimental realizations based on trapped ions in a linear Paul trap or stripline resonators on a square lattice. Using numerical and analytical methods, we have shown that the phase diagram is modified substantially. Compared to the original model with nn hopping only, the Mott lobe with density 1 becomes enlarged in the case of trapped ions but is reduced for the case of stripline resonators. This effect is particularly pronounced at selected chemical potentials in one dimension, due to the shape of the Mott lobe. In contrast, excitation spectra are only very weakly affected by the additional hopping terms, especially at low energies. In particular, the sound velocity at the lobe tip, as well as the universality class of the JCHM, remains unchanged.

An interesting problem arises from the possibility of tuning the hopping ratio t'/t in a circuit-QED setup. For $t' \gg t$, the lattice separates into independent, diagonal, 1D chains. By varying t'/t, one could thus observe a crossover from one to two dimensions, i.e., from Kosterlitz-Thouless behavior to mean-field-like behavior.

ACKNOWLEDGMENTS

We are grateful to F. Assaad, G. Blatter, A. Houck, J. Keeling, P. Pippan, and M. Troyer for useful discussions. This work made use of the ALPS applications [30]. M.H. was supported by DFG FG1162 and acknowledges the hospitality of ETH Zurich. L.P. was supported by the SNSF under Grant No. PZ00P2-131892/1.

APPENDIX: ATOMIC-LIMIT RESULTS

In the atomic limit ($t_{ij} = 0$) the eigenstates of Hamiltonian (1) are the dressed polariton states labeled by the polariton number n and upper/lower branch index $\sigma = \pm$. For $n > 0$ they can be written as a superposition of a Fock state with n photons plus atomic ground state $|n,\mathrm{g}\rangle$ and $(n-1)$ photons with the atom in its excited state $|(n-1),\mathrm{e}\rangle$,

$$\begin{aligned} |n+\rangle &= \sin\theta_n |n,\mathrm{g}\rangle + \cos\theta_n |(n-1),\mathrm{e}\rangle, \\ |n-\rangle &= \cos\theta_n |n,\mathrm{g}\rangle - \sin\theta_n |(n-1),\mathrm{e}\rangle, \end{aligned} \tag{A1}$$

where

$$\tan\theta_n = 2g\sqrt{n}/(\delta + 2\chi_n), \tag{A2}$$

with

$$\chi_n = \sqrt{g^2 n + \delta^2/4} \tag{A3}$$

and the detuning $\delta = \omega_\mathrm{b} - \omega_\mathrm{q}$. The eigenvalues are

$$\epsilon_n^\sigma = -(\mu - \omega_\mathrm{b})n - \delta/2 + \sigma\,\chi_n, \quad \sigma = \pm. \tag{A4}$$

The 0 polariton state $|0-\rangle = |0\,,g\rangle$ is a special case with $\epsilon_0^- = 0$. Upper and lower polariton energies are separated by the Rabi splitting $\Omega_n = 2\chi_n$. The spectral weights in Eq. (7) are then defined as

$$z_n^{\sigma,\sigma'} = \left(f_n^{\sigma,\sigma'}\right)^2, \tag{A5}$$

with the matrix elements $f_n^{\sigma,\sigma'} = \langle n\sigma|a^\dagger|(n-1)\sigma'\rangle$. The bare excitation energies are given by

$$\Delta_n^{\sigma,\sigma'} = \epsilon_n^\sigma - \epsilon_{n-1}^{\sigma'}. \tag{A6}$$

[1] M. Greiner *et al.*, Nature **415**, 39 (2002).
[2] M. P. A. Fisher, P. B. Weichman, G. Grinstein, and D. S. Fisher, Phys. Rev. B **40**, 546 (1989).
[3] J. Kasprzak *et al.*, Nature **443**, 409 (2006).
[4] A. D. Greentree, C. Tahan, J. H. Cole, and L. C. L. Hollenberg, Nat. Phys. **2**, 856 (2006).
[5] M. J. Hartmann, F. G. S. L. Brandão, and M. B. Plenio, Nat. Phys. **2**, 849 (2006).
[6] D. G. Angelakis, M. F. Santos, and S. Bose, Phys. Rev. A **76**, 031805(R) (2007).
[7] D. Rossini and R. Fazio, Phys. Rev. Lett. **99**, 186401 (2007).
[8] M. Aichhorn, M. Hohenadler, C. Tahan, and P. B. Littlewood, Phys. Rev. Lett. **100**, 216401 (2008).
[9] J. Zhao, A. W. Sandvik, and K. Ueda, e-print arXiv:0806.3603 (2008).
[10] J. Koch and K. Le Hur, Phys. Rev. A **80**, 023811 (2009).
[11] S. Schmidt and G. Blatter, Phys. Rev. Lett. **103**, 086403 (2009).
[12] S. Schmidt and G. Blatter, Phys. Rev. Lett. **104**, 216402 (2010).
[13] M. Knap, E. Arrigoni, and W. von der Linden, Phys. Rev. B **81**, 024301 (2010).
[14] M. Knap, E. Arrigoni, and W. von der Linden, Phys. Rev. B **82**, 045126 (2010).
[15] M. Hohenadler, M. Aichhorn, S. Schmidt, and L. Pollet, Phys. Rev. A **84**, 041608(R) (2011).
[16] N. Na, S. Utsunomiya, L. Tian, and Y. Yamamoto, Phys. Rev. A **77**, 031803(R) (2008).
[17] A. Nunnenkamp, J. Koch, and S. M. Girvin, New J. Phys. **13**, 095008 (2011).
[18] C.-W. Wu, M. Gao, Z. J. Deng, H. Y. Dai, P. X. Chen, and C. Z. Li, Phys. Rev. A **84**, 043827 (2011).
[19] P. Ivanov, S. S. Ivanov, N. V. Vitanov, A. Mering, M. Fleischhauer, and K. Singer, Phys. Rev. A **80**, 060301(R) (2009).
[20] A. Mering, M. Fleischhauer, P. A. Ivanov, and K. Singer, Phys. Rev. A **80**, 053821 (2009).
[21] T. D. Kühner and H. Monien, Phys. Rev. B **58**, R14741 (1998).
[22] J. Koch, A. A. Houck, K. L. Hur, and S. M. Girvin, Phys. Rev. A **82**, 043811 (2010).
[23] Y. Gao and F. Han, Mod. Phys. Lett. B **22**, 33 (2007).
[24] D. Jaksch, C. Bruder, J. I. Cirac, C. W. Gardiner, and P. Zoller, Phys. Rev. Lett. **81**, 3108 (1998).
[25] T. A. Zaleski and T. K. Kopec, J. Phys. B **43**, 085303 (2010).
[26] A. W. Sandvik, J. Phys. A **25**, 3667 (1992).
[27] P. Pippan, H. G. Evertz, and M. Hohenadler, Phys. Rev. A **80**, 033612 (2009).
[28] A. Albuquerque *et al.*, J. Magn. Magn. Mater. **310**, 1187 (2007).
[29] O. F. Syljuåsen and A. W. Sandvik, Phys. Rev. E **66**, 046701 (2002).
[30] F. Alet, S. Wessel, and M. Troyer, Phys. Rev. E **71**, 036706 (2005).
[31] L. Pollet, S. M. A. Rombouts, K. Van Houcke, and K. Heyde, Phys. Rev. E **70**, 056705 (2004).
[32] E. L. Pollock and D. M. Ceperley, Phys. Rev. B **36**, 8343 (1987).
[33] M. Potthoff, M. Aichhorn, and C. Dahnken, Phys. Rev. Lett. **91**, 206402 (2003).
[34] M. Knap, E. Arrigoni, and W. von der Linden, Phys. Rev. B **81**, 104303 (2010).
[35] W. Koller and N. Dupuis, J. Phys. Condens. Matter **18**, 9525 (2006).
[36] W. Metzner, Phys. Rev. B **43**, 8549 (1991).
[37] M. Ohliger and A. Pelster, e-print arXiv:0810.4399 (2008).
[38] M. J. Bhaseen, M. Hohenadler, A. O. Silver, and B. D. Simons, Phys. Rev. Lett. **102**, 135301 (2009).
[39] B. Capogrosso-Sansone, S. G. Söyler, N. Prokof'ev, and B. Svistunov, Phys. Rev. A **77**, 015602 (2008).